Review

Selection of a Suitable Wall Pressure Spectrum Model for Estimating Flow-Induced Noise in Sonar Applications

V. Bhujanga Rao
Naval Science and Technological Laboratory
Visakhapatnam 530 027, India

Flow-induced structural noise of a sonar dome in which the sonar transducer is housed, constitutes a major source of self-noise above a certain speed of the vessel. Excitation of the sonar dome structure by random pressure fluctuations in turbulent boundary layer flow leads to acoustic radiation into the interior of the dome. This acoustic radiation is termed flow-induced structural noise. Such noise contributes significantly to sonar self-noise of submerged vessels cruising at high speed and plays an important role in surface ships, torpedos, and towed sonars as well. Various turbulent boundary layer wall pressure models published were analyzed and the most suitable analytical model for the sonar dome application selected while taking into account high frequency, fluid loading, low wave number contribution, and pressure gradient effects. These investigations included type of coupling that exists between turbulent boundary layer pressure fluctuations and dome wall structure of a typical sonar dome. Comparison of theoretical data with measured data onboard a ship are also reported. © *1995 John Wiley & Sons, Inc.*

INTRODUCTION

The fluctuating pressure in the turbulent boundary layer is often termed pseudosound in recognition of the fact that it is essentially nonacoustic in nature and is also not associated with any significant far-field radiation if the wall is rigid, flat, and infinite. However, this pseudosound is quite real. It is the random forcing function that sets any underwater vehicle or its appendages like sonar domes into vibration with consequent acoustic radiation into the vehicle interior. Therefore, it is necessary to characterize this pseudosound in a suitable manner in order to estimate the interior noise levels.

Modeling of a turbulent wall pressure spectrum, that is, pseudosound, has been the subject of investigation for many years, but as of this date, no explicit model is available in the published literature for the full wave vector frequency spectrum of wall pressure fluctuations beneath turbulent boundary layers (Leehey, 1988; Hwang and Maidanik, 1990).

Received February 25, 1994; Revised March 24, 1995.
Shock and Vibration, Vol. 2, No. 5, pp. 403–412 (1995)

CCC 1070-9622/95/050403-10

TURBULENT BOUNDARY LAYER (TBL) WALL PRESSURE SPECTRUM MODELS

Corcos Model

According to Corcos (1964) the TBL wall pressure spectrum in wave number domain is given by

$$P(k_1, k_2, \omega) = \frac{P_p(o, \omega)\left[\alpha_1\alpha_2\left(\frac{\omega}{U_c}\right)^2\right]}{\left\{\pi^2\left[\left(k_1 - \frac{\omega}{U_c}\right)^2 + \left(\alpha_1\frac{\omega}{U_c}\right)^2\right]\left[k_2^2 + \left(\alpha_2\frac{\omega}{U_c}\right)^2\right]\right\}} \quad (1)$$

where ω/U_c is the convective wave number, and the point power spectrum $P_p(o, \omega)$ is given by

$$P_p(o, \omega) = \alpha_+(1 + \gamma)\rho_0^2 v_*^4/\omega \quad (2)$$

where ρ_0 is the fluid density, v_* is the friction velocity, U_c is the convective velocity, and a_+ and γ are constants. A set of constants suggested for use in the Corcos model are as follows:

$$\alpha_1 = 0.09, \quad \alpha_2 = 7\alpha_1, \quad a_+ = 0.766,$$

$$\gamma = 0.389, \quad \text{and } v_* = \sqrt{\frac{\tau_\omega}{\rho_0}}$$

where τ_ω is the wall shear stress.

It may be observed that the fit typically used in the Eq. (2) has a linear fall-off with frequency. In the limit $(k_1, k_2) \to (0, 0)$, $P(k_1, k_2, \omega)$ in Eq. (1) is approximately

$$P_p(0, \omega)\left(\frac{U_c}{\omega}\right)^2\left(\frac{\alpha_1}{\pi^2\alpha_2}\right).$$

This represents a low wave number level believed to be unrealistically high and it fails to exhibit the theoretically required $|\vec{k}|^2$ dependency in the low wave number region (Kraichnan, 1956; Chase, 1980; Ffowcs Williams, 1982). Davies (1971) conducted a series of experiments where a turbulent boundary layer excited a very thin rectangular panel that then radiated into a reverberant chamber surrounding the test section of his wind tunnel. Similarly Chang and Leehey (1976) carried out a series of analyses and experiments similar to that of Davies (1971), but for the case of an adverse pressure gradient. Comparison of these two experimental results with predictions based on the Corcos (1964) model for wall pressure statistics was later analyzed by Leehey (1988) and he drew the conclusion that the Corcos model overpredicts the low wave number components at a given frequency by as much as 13 dB.

Chase Models

In the derivation of the wave vector, frequency spectrum of wall pressure Chase (1980) considered contributions of both mean shear and pure turbulence to the spectrum of the wall pressure. In other words, this model includes the sum of interactions of each scale of motion with the mean flow as well as the self-interactions of eddies and the coupled interactions between different scales of motion. The desired form of the mean shear contribution to the wall pressure spectrum is given by

$$P_m(k_1, k_2, \omega) = \frac{C_m\rho_0^2 v_*^3 k_1^2}{\left[(\omega - k_1U_c)^2/(h_m v_*)^2 + \vec{k}^2 + \frac{1}{(b_m\delta)^2}\right]^{5/2}}; \quad (3)$$

and the desired form of the pure turbulence contribution to the wall pressure spectrum is given by

$$P_t(k_1, k_2, \omega) = \frac{C_t\rho_0^2 v_*^3 k^2}{\left[(\omega - k_1U_c)^2/(h_t v_*)^2 + \vec{k}^2 + \frac{1}{(b_t\delta)^2}\right]^{5/2}} \quad (4)$$

where $|\vec{k}|^2 = k^2 = k_1^2 + k_2^2$, δ is the boundary layer thickness, and C_m, C_t, h_m, h_t, b_m and b_t are constants. The sum of Eqs. (3) and (4) was suggested by Chase as an appropriate model of the wall pressure spectrum

$$P(k_1, k_2, \omega) = P_m(k_1, k_2, \omega) + P_t(k_1, k_2, \omega). \quad (5)$$

The constants C_m, C_t, h_m, and h_t are given by

$$C_t = \frac{3r_t a_+}{2\pi h_t}, \quad C_m = \frac{C_t + r_m}{r_t},$$

$$h_m = \frac{\mu_m U_c}{v_*}; \quad \text{and} \quad h_t = \frac{\mu_t U_c}{v_*} \quad (6)$$

where

$$r_t = 0.389, \quad r_m = 0.611, \quad a_+ = 0.766,$$
$$\mu_m = \mu_t = 0.176, \quad b_m = 0.765, \quad \text{and} \quad b_t = 0.378. \tag{7}$$

Constants for rough walls are given by Blake (1986) in his book. It should be noted that the simple specific model for the wave vector spectrum suggested in Eq. (5) is based on curve fitting of data with regard to diverse properties measured in wind tunnel experiments. Its validity for underwater application as far as the constants are concerned is under question.

All the experiments, used to fit the parameter values, such as Jameson (1975), Martin and Leehey (1977), and Farabee and Geib (1975) using either plates, membranes, or microphones as low wave number wave vector filters, are found to give upper bound values of the wall pressure spectrum that are remarkably low by most standards of practical interest in underwater acoustics. Chase (1980) explains that in underwater applications where this is so, the question is not what the level and dependence of low wave number wall pressure in those laboratory experiments are, but what the acoustic levels on propelled bodies in water having typical shapes, surface characteristics, and motions are. In the problem of excitation and radiation from the whole structure of an underwater body, the inhomogeneity and perhaps intensification associated with the region of flow transition on these bodies may yield low wave number levels that are higher and hence also play a significant role.

Chase (1987) also suggested wave vector pressure spectrum models for both subconvective and radiative domains where the source model of Chase (1980) offers a general treatment of the wave vector frequency spectrum of a turbulent boundary layer without specific reference to convective, subconvective, or acoustic domains.

Ffowcs Williams Model

Ffowcs Williams (1982) extended the Corcos model to make it applicable to the low wave number elements of the spectrum as required in the case of underwater applications. Starting with Lighthill's acoustic analogy and his own earlier paper (1965), Ffowcs Williams proposed the following representation for the wall pressure spectrum:

$$P_p(\vec{k}, \omega) = \rho_0^2 U_\infty^3 b^{*3} P_0\left(\frac{\omega\delta^*}{U_\infty}\right) A_0\left(1 - \frac{k_1 U_c}{\omega}\right) B_0\left(\frac{k_2 U_c}{\omega}\right) \left\{ a_0\left(\frac{U_c|\vec{k}|^2}{\omega}\right) + a_1 M^2 + a_2 M^4 \ln(R/\delta^*)\delta\left[\left(\frac{U_\infty|\vec{k}|}{\omega}\right)^2 - M^2\right]\right\} \tag{8}$$

where ρ_0 is the density of the fluid, δ is the Dirac delta function, and $M = U_\infty/C$. The functions P_0, A_0, B_0, and the constants a_0, a_1, and a_2 must be determined by experiments. The last term in Eq. (8) represents the acoustically coincident elements of the spectrum. Hence, R denotes the effective extent of the turbulence zone that contributes to the energy at $k^2 = w^2/C^2$.

Hwang and Maidanik Model

The Corcos model applies in the neighborhood of the convective region, whereas the Chase model agrees well with the data over a broader range of wave numbers. But the convenient form of the Corcos model, however, motivates attempts to extend its range of validity to lower wave numbers as more experimental data are obtained. Hwang and Maidanik suggested a model that is analytically simple like Corcos and at the same time follows the theoretical requirement of $|k^2|$ dependence in the low wave number region as in Chase model. Equation (9) indicates this model as given below:

$$P(\vec{\xi}, \omega) = P_p(\omega) A\left(\frac{\omega\xi}{U_c}\right) B\left(\frac{\omega\eta}{U_c}\right)$$
$$A\left(\frac{\omega\xi}{U_c}\right) = \exp^{-a_1|\omega\xi/U_c|}\exp^{i(\omega\xi/U_c)} \tag{9}$$
$$B\left(\frac{\omega\eta}{U_c}\right) = \exp^{-a_2|\omega\eta/U_c|}$$

when $P_p(\omega)$ is the frequency spectrum, U_c is the convective velocity, and a_1 and a_2 are decaying constants that have a typical range of values 0.11–0.12 and 0.7–1.2, respectively, for a smooth rigid wall.

Christoph Model: Modified Corcos Model Without Pressure Gradient Effects

Christoph (1987) modeled wall pressure frequency spectrum differently from that given by

the original Corcos model. This was done by nondimensionalizing experimental data with different flow variables and by more accurately curve fitting the resulting nondimensional frequency spectra.

The curve used in this study to model the data is

$$P(\omega) = \frac{3\tau_\omega^2 \delta^*}{U_\infty[1 + (\omega\delta^*/U_\infty)^2]}, \tag{10}$$

which is used for both smooth and rough surfaces. The fit typically used with the Corcos model is

$$P(\omega) = \rho^2 v_*^4/\omega. \tag{11}$$

It can be seen that Eq. (11) has a linear fall-off with frequency. It is felt that the present wall pressure frequency spectrum model, eq. (10), more universally fits smooth and rough wall flows and that the high frequency fall-off is in better agreement with the data. Equation (10), which is a frequency spectrum, should be used in Eq. (1) for getting the final wave number spectrum as given below:

$$P(k_1, k_2, \omega) = \frac{P(\omega)}{\pi}\left[\frac{ak_c}{(ak_c)^2 + (k_1 - k_c)^2}\right]\left[\frac{bk_c}{(bk_c)^2 + k_2^2}\right] \tag{12}$$

where k_c is the convective wave number.

Several observations can be made from the Christoph modification of the Corcos model. First, the convective peak has shifted to higher wave numbers. This is simply a result of the lower convective velocity. The convective peak has also broadened. More energy has shifted to the lower and higher wave numbers.

Christoph Model: Modified Corcos Model With Pressure Gradient Effects

All the above models are based on smooth, flat plates and zero pressure gradient data. Undersea vehicles have pressure gradients. Based on the experimental data of Corcos (1964), Schloemer (1966), and Burton (1973), the wall pressure model was modified by Christoph (1989) to include fluid-injection and pressure gradients. Because we are interested in pressure gradient effects only, fluid injection effects will not be discussed here.

The flow noise model for pressure gradients is based on experimental data from Burton (1973) and Schloemer (1966). Both experiments were conducted in subsonic wind tunnels. Burton considered both smooth and rough walls in adverse and favorable pressure gradients. Flow separation was approached in the severe adverse gradient. Schloemer studied mild adverse and favorable gradients. Christoph's (1989) modeling effort concentrated on adverse gradients as the case of most interest. Both Burton and Schloemer found that adverse gradients showed convective velocities and increased longitudinal spatial decay rates. Burton also reported that the total power in the wall pressure signal remained independent of pressure gradient, distributing itself from higher to lower frequencies. Burton (1973) noted that root mean square wall pressures were nearly independent of pressure gradients.

Christoph (1989) estimated boundary layer parameters in order to nondimensionalize the wall pressure frequency data of Schloemer (1966) and Burton (1973). It was found that this nondimensionalization adequately collapsed the pressure gradient data into a single curve. The curve fit used in the fall-off frequency range is

$$P(\omega) = \frac{P(0)}{[1 + (\omega\delta^*/U_\infty)^2]}\left[\frac{q^2\delta^{*^2}}{U_\infty\delta_0^*}\right]. \tag{13}$$

The convective velocity U_c was approximated as

$$U_c/U_\infty = 0.6\left[1.0 - 15\frac{\delta^*}{q}\frac{dP}{dx}\right] \tag{14}$$

and the parameter a_1 in the original Corcos (1964) model as

$$a = 0.9\left[1.0 - 0.15\frac{\delta^*}{q}\frac{dP}{dx}\right] \tag{15}$$

where $q = \frac{1}{2}\rho_0 U_\infty^2$.

Josserand and Lauchle Model

Josserand and Lauchle (1990) derived certain semiempirical formulae from vast measurements of the space–time correlation function for the formation, convection, and coalescence of turbulent spots in a naturally occurring flat plate boundary layer transition zone. The spot statistics were coupled with the Chase (1980) model for turbulent

boundary layer wall pressure statistics to arrive at a model for the transition region wall pressure wave vector frequency spectrum. Although the transition region has been reported to be an intense source of underwater noise, this model of Josserand and Lauchle, which is most valid in the convective domain (high wave number spectral domain), is not discussed further here.

SONAR DOME: A CASE STUDY

To identify a suitable wave vector spectrum model for underwater application, a case study of a sonar dome was considered in this article. A sonar dome that houses the sonar transducer responds to flow excitation, and the radiated structural noise is received by the sonar transducer as self-noise due to flow. Bhujanga Rao (1987, 1992) reports a number of experiments conducted onboard a typical ship. That data has been used in the article to select the suitable model for a wall pressure spectrum.

WAVE NUMBER ANALYSIS OF MODE COUPLING BETWEEN SONAR DOME STRUCTURE AND PRESSURE FIELD OF FLOW TURBULENCE

It is known that the degree of power reception by a structure excited by a spatially and temporally random pressure field depends on how well the structure spatially filters out excitation wave numbers.

The sonar dome has been assumed as consisting of two parallel rectangular plates of length 'a' and breadth 'd' as shown in Figure 1. The theoretical and experimental justification for such idealization is discussed in detail by Bhujanga Rao (1992).

The coupling coefficient $J_{mn}(\omega)$ of a structural mode and the turbulent boundary layer pressure field is defined to be the ratio of the modal force spectral density, and the total pressure force density, as given in Hwang and Maidanik (1990). To determine the relative contributions to the couplings by various wave number regions, the three regions are defined as follows:

1. a low wave number region covering $\omega/c < k_1 \leq 0.2\omega/U_c$;
2. the high wave number region centered at the hydrodynamic coincidence and covering a range $0.5\omega/U_c \leq k_1 \leq 1.5\omega/U_c$;
3. the intermediate wave number region lying between the two regions just defined, i.e., $0.2\omega/U_c < k_1 \leq 0.5\omega/U_c$.

Let the contribution to the coupling by the low, intermediate, and high wave number regions be designated as $J^L_{mn}(\omega)$, $J^I_{mn}(\omega)$, and $J^H_{mn}(\omega)$, respectively. It follows that the total nonacoustic contribution to the coupling is the sum of the above three factors, i.e.,

$$J_{mn}(\omega) = J^L_{mn}(\omega) + J^I_{mn}(\omega) + J^H_{mn}(\omega). \quad (16)$$

Equations (17), (18), and (19) give the expressions as derived by Hwang and Maidanik (1990) for $J^L_{mn}(\omega)$, $J^I_{mn}(\omega)$, and $J^H_{mn}(\omega)$, respectively.

$$J^L_{mn}(\omega) \simeq \overline{\Delta k_1}\,\overline{\Delta k_2}\,\overline{\psi}^2_{mn} G_m(\bar{k}_m) G_n(\bar{k}_n)$$

where

$$\overline{\Delta k_1} = \frac{(2\pi/a)}{(\omega/U_c)},$$

$$\overline{\Delta k_2} = \frac{(2\pi/b)}{(\omega/U_c)}, \quad (17)$$

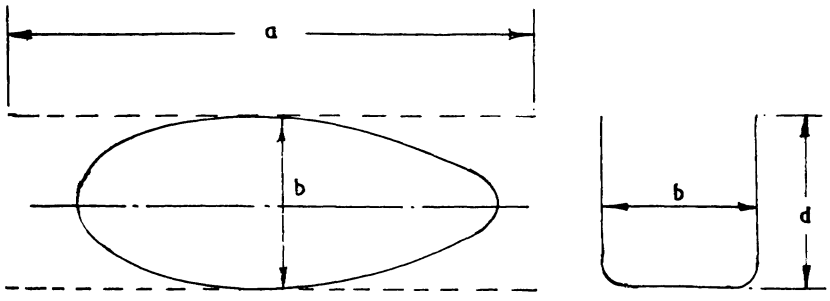

FIGURE 1 Idealization of curved dome wall as two equivalent flat plates of length 'a' and breadth 'b'.

$$J^{I}_{mn}(\omega) = (\overline{\Delta k_1})(\overline{\Delta k_2})\overline{\psi}^2_{mn}\left\{\frac{2\alpha_1\alpha_2}{\pi^2}\left[\frac{1}{4}+\frac{\ln m}{2m}\bar{k}_n^2 + \left(\frac{6.6}{m}\right)\bar{k}_m^3\right]\right\} G_2(\bar{k}_n) \quad (18)$$

$$J^{H}_{mn}(\omega) \simeq (\overline{\Delta k_1})(\overline{\Delta k_2})\overline{\psi}^2_{mn}\left\{\frac{55\alpha_1\alpha_1\bar{k}_m^3}{m\pi^3}\right\} G_2(\bar{k}_n) \quad (19)$$

where $\overline{\psi}^2_{mn}$ is by definition, the spatial mean square value of the mode function.

Curves drawn in Figure 2 for first four modes show that the coupling of turbulent boundary layer flow field with the structure is maximum in the low wave number region. With boundary conditions such as clamped or free coupling of the pressure field with structural response will remain unaffected (Hwang and Maidanik, 1990).

SELECTION OF SUITABLE WAVE VECTOR SPECTRUM MODEL FOR SONAR APPLICATION

As already discussed, Corcos (1964) suggested the first model of the wave number frequency spectrum based on similarity principles. The Corcos model has two major limitations: it does not account for the effects of compressibility that control the sonic and supersonic phase velocity range of the spectrum; and it violates the $|k|^2$ dependence of the spectrum at low wave numbers as theory demands. Wind tunnel measurements

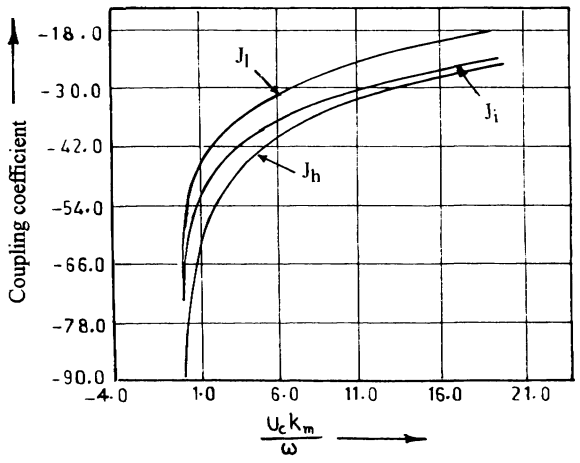

FIGURE 2 Mode Coupling between sonar dome wall and excitation pressure field J_l, J_i, J_h indicate coupling of low, intermediate, and high wave numbers respectively. Ka = 82.46; m = 4.

indicate the Corcos model overpredicts the spectrum levels at low wave numbers.

The positive aspects that attract any investigator for use of Corcos model follow:

Available low wave number wall pressure data, whether done with microphone arrays or mechanical plate filters, indicate wave number white spectrum, beginning at a wave number substantially above the acoustic wave number. There is no indication that the incompressible $|k|^2$ low wave number limit of Kraichnan (1956) is approached in any way in practice. Measurements taken in two dissimilar wind tunnels, one at MIT by Martini, Leehey, and Moeller (1984) and one at David Taylor Naval Ship Research and Development Centre (DTNSRDC) by Farabee and Geib (1975) with very low background noise levels, confirm quite similar results with wave number white spectra characteristic in the low wave number region. However, measurements taken by Jameson (1975) at Bolt Beranak and Newman wind tunnel indicate significantly lower levels of low wave number spectra. This discrepancy has defied repeated efforts at explanation. It is possible that in both MIT and DTNSRDC experiments, however low the tunnel noise, suffer from acoustic contamination of data that the wave number white behavior reflects wind tunnel facility noise contamination. Leehey (1988) in his review feels that it is also possible that these results are inherent to the boundary layer itself: from the mechanism of radiation by oscillatory wall shear or perhaps by radiation from the trailing edge portion of the test plates. Further, according to Leehey such mechanisms are always possible and likely to be inherent to any practical application of the wall pressure data to structural response problems. He considers it prudent that current practice is to use a model of the wall pressure spectrum that incorporates a wave number white region for wave number appreciably below those of the convective range irrespective of theoretical violations.

The Corcos model is analytically simple and easy to use as a forcing function to arrive at closed form solutions for structural response problems.

Perhaps for the reasons mentioned above, the Corcos model has been modified to include effects of pressure gradients, variation in fall-off with frequency, fluid injection, etc. On the other hand, Chase (1980, 1987) models that encompass all wave number domains including radiative domain mainly suffers from the following disadvantages: Although based on sound theoretical considera-

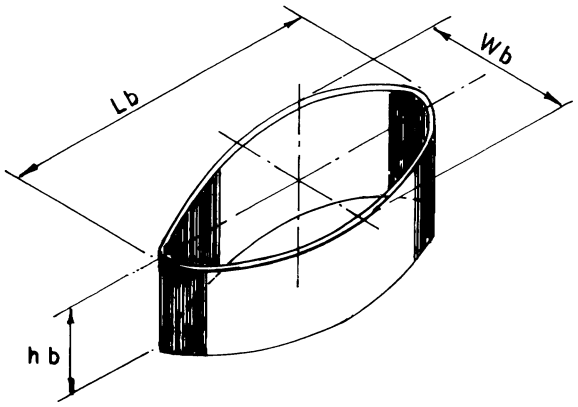

FIGURE 3 Sonar dome configuration.

tions and satisfying the necessary $|k|^2$ dependence at low wave numbers, it offers unrealistically low pressure levels compared to practical data in underwater acoustics. Parameter values have not been adequately proved against underwater experiments. Data from wind tunnel experiments have been used throughout the validation of the Chase models. The models have not been extended either by Chase or others for inclusion of pressure gradient, mass injection effects, etc., for analyzing bodies of more practical interest.

The sonar dome, whose configuration is shown in Figure 3 being an appendage of practical underwater interest, the following wave vector model formulation has been used for theoretically computing interior acoustic response, i.e., flow-induced structural noise of the dome.

Favorable and Zero Pressure Gradient Region of Dome

In this region, the Corcos (1964) model as modified by Christoph (1987) for obtaining better high frequency fall-off corresponds to the frequency range of sonar interest.

Adverse Pressure Gradient Region of Body

In this region, the Corcos (1964) model as modified by Christoph (1989) included adverse pressure gradient effects. Figures 4, 5, and 6 give details of the forcing function estimated using various models, namely the Corcos (1964), Christoph

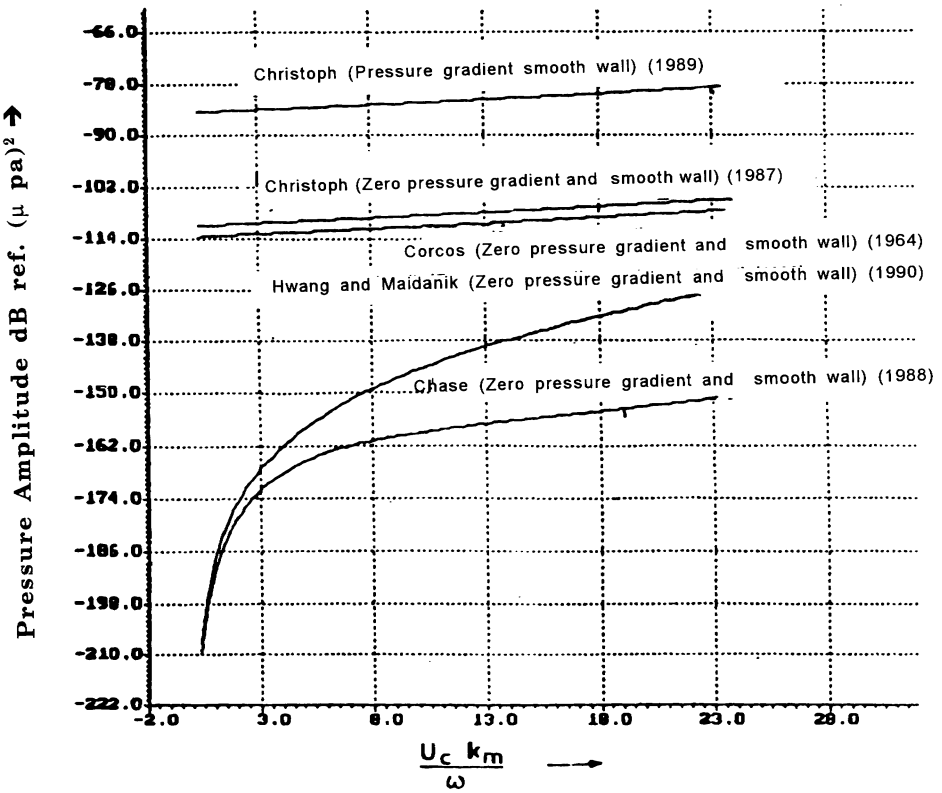

FIGURE 4 Turbulent boundary layer excitation pressure amplitude as a function of non-dimensional wave number at 15% dome length.

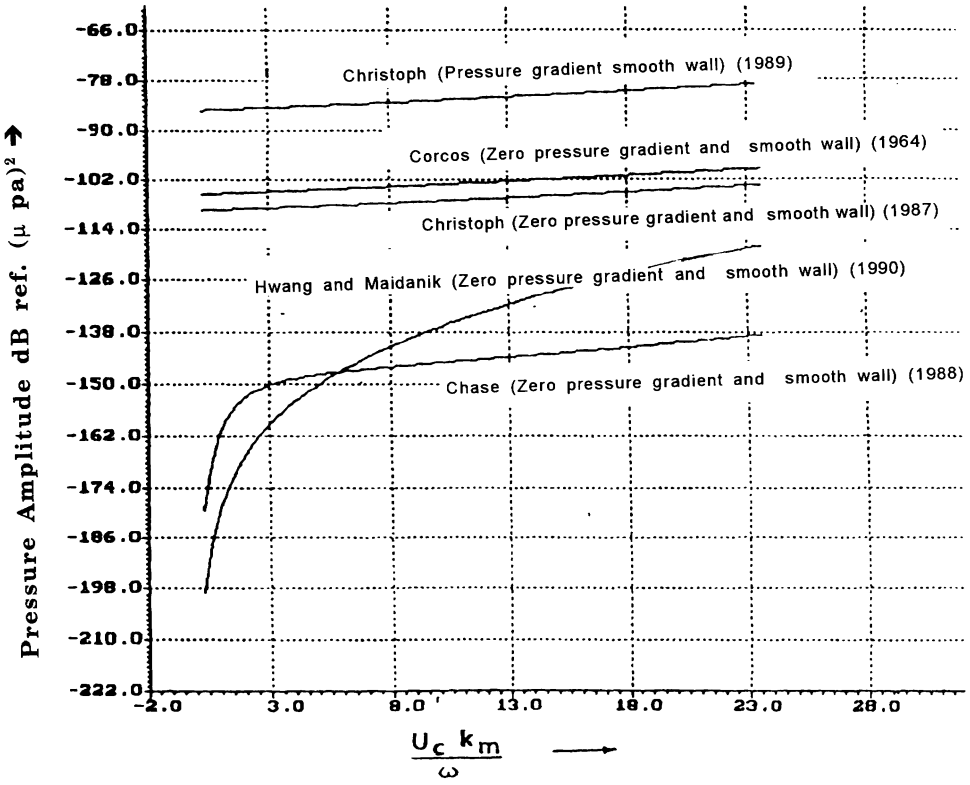

FIGURE 5 Turbulent boundary layer excitation pressure amplitude as a function of non-dimensional wave number at 50% dome length.

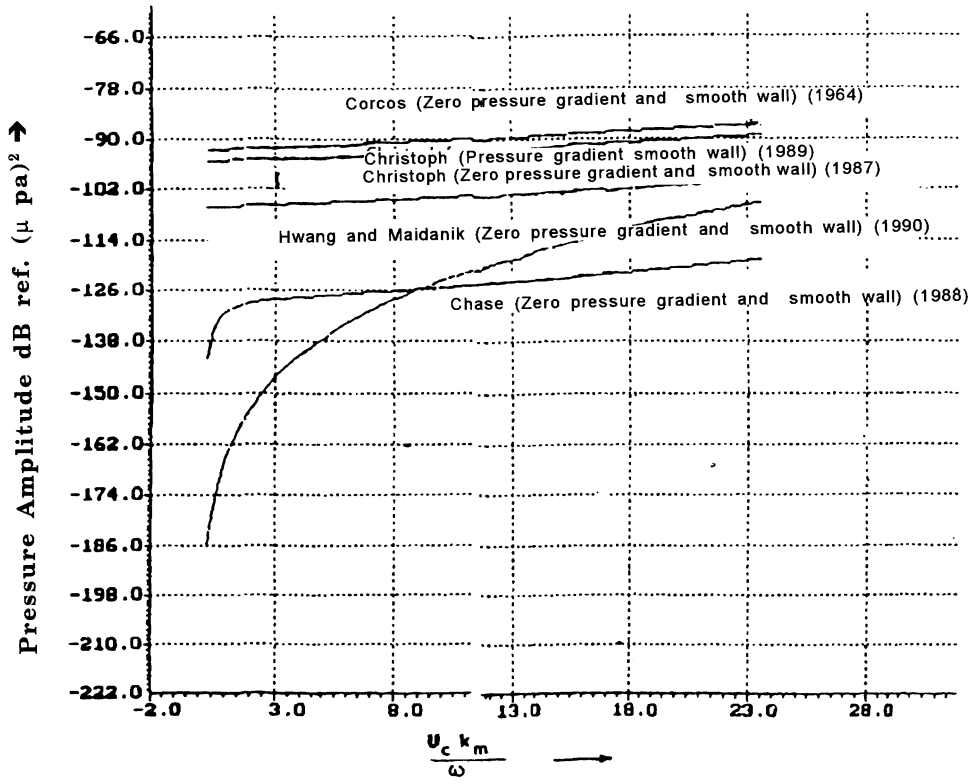

FIGURE 6 Turbulent boundary layer excitation pressure amplitude as a function of non-dimensional wave number at 75% dome length.

smooth wall without pressure gradient effects (1987), Christoph smooth wall with pressure gradient effects (1989), and Chase (1987) and Hwang and Maidanik (1990) in the range of wave numbers lying between $\omega/c < k < 0.3\omega/U_c$ at three different stations on the sonar dome body at a speed of 10 m/s. It may be seen from this figure that the Corcos (1964) and Christoph (1987, 1989) models are wave vector white whereas that of Chase and Hwang and Maidanik follow $|k|^2$ dependence.

The acoustic pressure levels computed theoretically using these selected models were compared with practical experimental data obtained under controlled experiments onboard a ship and found to show good agreement as shown in Figures 7 and 8 at two different speeds.

RESULTS AND DISCUSSION

Although the Corcos (1964) and Christoph (1987, 1989) models used in the estimation of flow-induced structural noise are not low wave number models, the results shown in Figures 7 and 8 are surprisingly in good agreement. This reinforces the argument by Leehey (1988) that the low wave number limit of Kraichnan (1956) is not approached in any way in practice.

The models used, being intrinsically wave number white, are sufficient to predict the flow noise in underwater applications.

Although the Davies (1971) experiment in the wind tunnel indicated that the Corcos (1964) model overpredicts the results by 13 dB, it is not seen when applied to the underwater case of sonar dome. It is, therefore, prudent to conduct more experiments underwater.

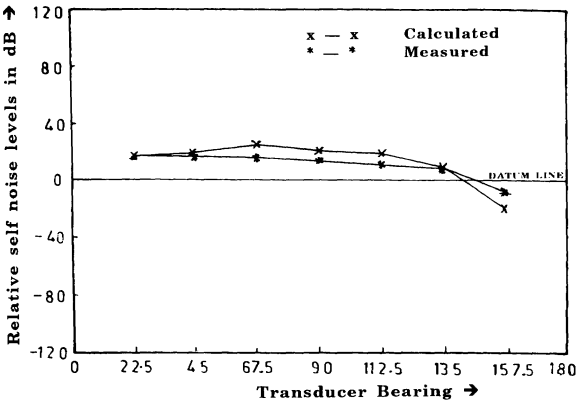

FIGURE 7 Comparison of theoretical and measured levels at different bearings—at speed 10 m/sec.

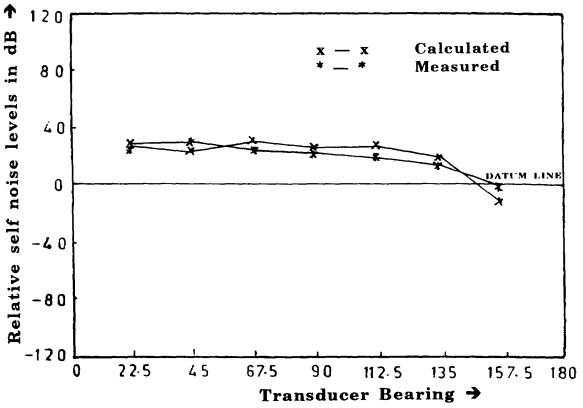

FIGURE 8 Comparison of theoretical and measured levels at different bearings—at speed 11.5 m/sec.

Chase models, which are intrinsically very good models from a theoretical point of view, need to be validated against underwater experiments and the constants such as C_m, C_t, h_m, h_t, etc., are to be evaluated.

REFERENCES

Bhujanga Rao, V., 1987, "On the Flow-Induced Structural Noise of a Ship's Sonar Dome," *Journal of Marine Technology and SNAME News, USA,* 24, 321–331.

Bhujanga Rao, V., 1992, "Flow-Induced Acoustic Response Modelling of a Ship's Sonar Dome," Report No. VBR, August.

Blake, W. K., 1986, *Mechanics of Flow-Induced Sound and Vibration,* Vol. II, Academic Press, Orlando, FL.

Burton, T. E., 1973, "Wall Pressure Fluctuations at Smooth and Rough Surfaces Under Turbulent Boundary Layers with Favourable and Adverse Pressure Gradients," Acoustics and Vibration Laboratory, MIT, Report No. 70208-9.

Chang, Y. M. and Leehey, P., 1976, "Vibration of Noise and Acoustic Radiation from a Panel Excited by Adverse Pressure Gradient Flow," Acoustics and Vibration Laboratory, MIT, Report No. 70208-12.

Chase, D. M., 1980, "Modelling the Wave Vector-Frequency Spectrum of Turbulent Boundary Layer Wall Pressure," *Journal of Sound and Vibration,* 70, 29–67.

Chase, D. M., 1987, "The Characteristics of the Turbulent Wall Pressure Spectrum at Subconvective Wave Numbers and a Suggested Comprehensive Model," *Journal of Sound and Vibration,* 112, 125–147.

Christoph, G. H., 1987, "Surface Roughness Effects on Flow Noise," 114th Meeting of the Acoustical Society of America, *Journal of Acoustical Society of America,* Vol. 82, Suppl. 1, S27.

Christoph, G. H., 1989, "Fluid Injection and Pressure Gradient Effects on Flow Noise," Paper presented at the 117th Meeting of the Acoustical Society of America, *Journal of Acoustical Society of America,* 85, Suppl. 1, S3.

Corcos, G. M., 1964, "The Structure of the Turbulent Pressure Field in Boundary Layer Flows," *Journal of Fluid Mechanics.*

Davies, H. G., 1971, "Sound from Turbulent Boundary Layer Excited Panels," *Journal of Acoustical Society of America,* 49, 878–889.

Farabee, T. M. and Geib, F. E., Jr., 1975 and 1976, "Measurement of Boundary Layer Pressure Fields with an Array of Pressure Transducers in a Subsonic Flow," 6th International Congress of Instrumentation in Aerospace, Ottawa, Canada.

Ffowcs Williams, J. E., 1982, "Boundary Layer Pressures and Corcos Model: A Development to Incorporate Low Wave Number Constraints," *Journal of Fluid Mechanics,* 125, 9–25.

Hwang, Y. F. and Maidanik, G., 1990, "A Wave Number Analysis of the Coupling of a Structural Mode and Flow Turbulence," *Journal of Sound and Vibration,* 142, 135–152.

Jameson, P. E., 1975, "Measurement of the Low-Wave Number Component of Turbulent Boundary Layer Pressure Spectral Density," 4th Biennial Symposium on Turbulence in Liquids, Sept. 22–24, Rolla, MO.

Josserand, M. A. and Lauchle, G. C., 1990, "Modeling the Wave Vector Frequency Spectrum of Boundary Layer Wall Pressure During Transition on a Flat Plate," *Journal of Vibration and Acoustics,* 112, 523–534.

Kraichnan, R. H., 1956, "Pressure Fluctuations in Turbulent Flow over a Flat Plate," *Journal of Acoustical Society of America,* 28, 378–390.

Leehey, P., 1988, "Structural Excitation by a Turbulent Boundary Layer: An Over-view," *Journal of Vibration, Stress and Reliability in Design,* 110, 220–225.

Martin, N. C. and Leehey, P., 1977, "Low Wave Number Wall Pressure Measurements Using a Rectangular Membrance as a Spatial Filter," *Journal of Sound and Vibration,* 52, 95–120.

Martini, K., Leehey, P., and Moeller, M., 1984, "Comparison of Techniques to Measure the Low Wave Number Spectrum of a Turbulent Boundary Layer," Acoustics and Vibration Laboratory, MIT, Report No. 92828-1.

Schloemer, H. H., 1966, "Effects of Pressure Gradients on Turbulent Boundary Layer Wall Prerssure Fluctuations," *Journal of Acoustical Society of America,* 42, 93–113.